

Thermal explosion simulation and incompatible reaction of dicumyl peroxide by calorimetric technique

Sun-Ju Shen · Sheng-Hung Wu · Jen-Hao Chi ·
Yih-Wen Wang · Chi-Min Shu

NATAS2009 Special Issue
© Akadémiai Kiadó, Budapest, Hungary 2010

Abstract Dicumyl peroxide (DCPO) is usually employed as an initiator for polymerization, a source of free radicals, a hardener, and a linking agent. In Asia, due to its unstable reactive nature, DCPO has caused many thermal explosions and runaway reaction incidents in the manufacturing process. This study was conducted to elucidate its essentially thermal hazard characteristics. In order to analyze the runaway behavior of DCPO in a batch reactor, thermokinetic parameters, such as heat of decomposition (ΔH_d) and exothermic onset temperature (T_0), were measured via differential scanning calorimetry (DSC). Thermal runaway phenomena were then thoroughly investigated by DSC. The thermokinetics of DCPO mixed with acids or bases were determined by DSC, and the experimental data were compared with kinetics-based curve fitting of thermal safety

software (TSS). Solid thermal explosion (STE) and liquid thermal explosion (LTE) simulations of TSS were applied to determine the fundamental thermal explosion behavior in large tanks or drums. Results from curve fitting indicated that all of the acids or bases could induce exothermic reactions at even an earlier stage of the experiments. In order to diminish the extent of hazard, hazard information must be provided to the manufacturing process. Thermal hazard of DCPO mixed with nitric acid (HNO_3) was more dangerous than with other acids including sulfuric acid (H_2SO_4), phosphoric acid (H_3PO_4), and hydrochloric acid (HCl). By DSC, T_0 , heat of decomposition (ΔH_d), and activation energy (E_a) of DCPO mixed with HNO_3 were calculated to be 70 °C, 911 J g⁻¹, and 33 kJ mol⁻¹, respectively.

Keywords Dicumyl peroxide (DCPO) ·
Differential scanning calorimetry (DSC) ·
Liquid thermal explosion (LTE) ·
Solid thermal explosion (STE) ·
Thermal hazard characteristics

S.-J. Shen
Department of Occupational Safety and Health, Chia Nan
University of Pharmacy and Science, 60, Erh-Jen Rd., Sec. 1,
Jente, Tainan 71710, Taiwan, ROC

S.-H. Wu · J.-H. Chi
Department of Fire Science, WuFeng Institute of Technology,
117, Chian-Kuo Rd., Sec. 2, Min-Hsiung, Chiayi 62153, Taiwan,
ROC
e-mail: wushprofessor@gmail.com

Y.-W. Wang
Department of Occupational Safety and Health, Jen-Teh Junior
College of Medicine, Nursing and Management, 1, Jen-Teh Rd.,
Houlong, Miaoli 65601, Taiwan, ROC

S.-J. Shen · C.-M. Shu (✉)
Graduate School of Engineering Science and Technology,
National Yunlin University of Science and Technology
(NYUST), 123, University Rd., Sec. 3, Douliou, Yunlin 64002,
Taiwan, ROC
e-mail: shucm@yuntech.edu.tw

Abbreviations

A	Frequency factor (s ⁻¹ M ¹⁻ⁿ)
A_{tot}	Total peak area (mJ)
C_p	Liquid specific heat at constant pressure (kJ kg ⁻¹ °C ⁻¹)
E_a	Activation energy (kJ mol ⁻¹)
H	The DSC signal deviation from baseline (mW)
k	Reaction rate (s ⁻¹)
k_0	Reaction rate of initiation (s ⁻¹)
M	Mass of reactant (mg)
n	Reaction order (dimensionless)
Q	Calorific capacity (J g ⁻¹)
R	Ideal gas constant (8.314 J mol ⁻¹ K ⁻¹)

SADT	Self-accelerating decomposition temperature (°C)
T	Temperature of reaction (°C)
T_0	Exothermic onset temperature (°C)
T_e	Environmental temperature (°C)
T_c	Critical temperature (°C)
T_{\max}	Maximum temperature during overall reaction (°C)
T_{NR}	Temperature of no return (°C)
T_{wall}	Temperature on the wall (°C)
HTC	Heat transfer coefficient ($\text{W m}^{-2} \text{K}^{-1}$)
α	Degree of conversion (dimensionless)
β	Heating rate ($^{\circ}\text{C min}^{-1}$)
ΔH_d	Heat of decomposition (J g^{-1})
λ	Thermal conductivity (J ms K^{-1})

Introduction

The widespread use of chemicals in the manufacturing process poses a high risk of illness, injury, disablement, and even death. According to statistics, most chemical accidents are due to poor training, insufficient warning signs, and inadequate material safety data sheet (MSDS) information as from accident investigation. Therefore, the United Nations (UN) structured a series system as a common standard worldwide that was named the Globally Harmonized System of Classification and Labelling of Chemicals (GHS).

Accident rate, illness rate, and incident rate of chemicals in Taiwan are of a higher percentage than in Japan, the USA, and the UK. Especially, the accident rate of explosive materials is higher than others chemicals. The aim of this study was focused on organic peroxides (OPs) that were demonstrated as Division 5.2 in GHS. OPs, which can exothermically decompose, require inherently safe design during preparation, manufacturing, transportation, storage, and even disposal. They can release tremendous amounts of thermal energy and result in high pressure during runaway excursion, leading to fire, explosion, or toxic release [1–13]. According to Table 1, three accidents have caused thermal explosions and runaway reactions by dicumyl peroxide (DCPO) in a batch reactor in Japan and Taiwan.

DCPO ($\text{C}_{18}\text{H}_{22}\text{O}_2$), one of the OPs, has caused several thermal explosions and runaway reactions because of its unstable peroxy bonds ($-\text{O}-\text{O}-$). DCPO is white solid under room temperature and widely employed as initiator and cross-linking agent for polyethylene (PE), ethylene vinyl acetate (EVA) copolymer, ethylene propylene terpolymer (EPT), and as a curing agent for unsaturated polystyrene (PS). Small-scale tests (laboratory testing, research for department of research and development

Table 1 Selected thermal explosion incidents caused by CHP and DCPO in Japan and Taiwan

Year	Chemical	Location	Deaths/Injuries	Hazard
1981	CHP	Taiwan	1/3	Explosion ^a
1986	CHP	Taiwan	0/0	Explosion ^b
1988	DCPO	Japan	0/1	Explosion ^b
1999	DCPO	Taiwan	0/0	Explosion ^b
2003	CHP/DCPO	Taiwan	0/2	Explosion ^b
2005	DCPO	Taiwan	0/0	Explosion ^b
2008	DCPO	Taiwan	0/0	Explosion ^b
2010	CHP	Taiwan	0/0	Explosion ^c

^a Storage; ^b Reactor; ^c Oxidation tower

(R&D) etc.) are necessary and mandatory for loss prevention and damage control.

Differential scanning calorimetry (DSC) was applied to determine the fundamental parameters including exothermic onset temperature (T_0), activation energy (E_a), and heat of decomposition (ΔH_d). The explosion and reaction development simulations are useful and successful technologies for practical situations in industries. The thermokinetics of DCPO was determined by DSC, and the experimental data were compared with kinetics-based curve fitting of thermal safety software (TSS). Solid thermal explosion (STE) and liquid thermal explosion (LTE) simulations of TSS were applied to determine the fundamental thermal explosion behavior in large tanks or drums [14].

Acids (including nitric acid (HNO_3), sulfuric acid (H_2SO_4), phosphoric acid (H_3PO_4), and hydrochloric acid (HCl)), and bases (involving sodium hydroxide—NaOH) and potassium hydroxide—KOH) are widely used as catalysts and reactants in chemical industries. For instance, H_2SO_4 is applied to catalyze cumene hydroperoxide (CHP) producing phenol and acetone [12] in chemical industries. Cumene, CHP, cumyl alcohol (CA), and H_2SO_4 are applied to manufacture DCPO in the batch reactor [11]. In parallel, a few of DCPO can be produced and can be mixed with H_2SO_4 in the reactor [11]. Besides, NaOH is usually being used as neutralizer when H_2SO_4 is added over process design, with the temperature increasing suddenly [15]. Therefore, DCPO can be mixed with those acids and bases at normal or abnormal situation. Consequently, incompatible reaction should be studied to ensure the operational safety in the chemical industries.

Results from curve fitting indicated that all of the acids or reactor could induce exothermic reactions at even an earlier stage of the experiments. In order to diminish the extent of the hazard, thermal hazard information must be provided to the manufacturing process. Thermal hazard of nitric acid (HNO_3) mixed with DCPO was more dangerous

than with other acids including sulfuric acid (H_2SO_4), phosphoric acid (H_3PO_4), and hydrochloric acid (HCl). The T_0 , ΔH_d , and E_a of DCPO mixed with 6 N HNO_3 were calculated to be $70\text{ }^\circ\text{C}$, 911 J g^{-1} , and 33 kJ mol^{-1} , respectively.

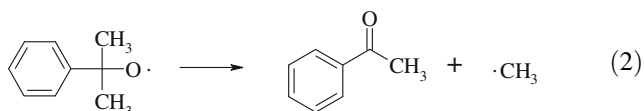
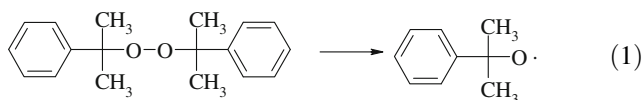
Experimental

Samples

The DCPO of 99 mass% was directly purchased from the Fluka Co., and both density and concentration were measured. DCPO is a solid material and was stored at room temperature in moisture-proof box. The melting point of DCPO was determined to be $40\text{ }^\circ\text{C}$.

According to Eq. 1, this study has provided the significant phenomenon. At the vulcanization temperature, DCPO, when decomposed homiletically in nonacid medium, will produce cumyloxy radicals.

In the meantime, these radicals were quite unstable. Consequently, Eq. 2 was applied to describe the reaction mechanisms as methyl radical and acetophenone producing. Either the cumyloxy radical or the methyl radical abstracts a hydrogen atom from the polymer, mainly from the carbon atom indicated [11].



for incompatible reaction determination, HNO_3 , H_2SO_4 , H_3PO_4 , HCl , NaOH , and KOH were prepared as 6 N of concentration.

Differential scanning calorimetry

Dynamic scanning experiments were executed on a Mettler TA8000 system coupled with a DSC 821^e measuring test crucible (Mettler ME-26732), which is the essential part of the experiment. It was used to perform experiments for withstanding relatively high pressure of approximately 100 bar.

Temperature-programmed screening experiments were performed with DSC. The heating rates (β) selected for the temperature-programmed ramp were 1, 2, 4, and $10\text{ }^\circ\text{C min}^{-1}$. The range of temperature rise was chosen from 30 to $300\text{ }^\circ\text{C}$ for 99.3 mass% DCPO.

DSC was used to detect the temperature change between the sample and reference for determining the heat change, time, and temperature. Roughly 3–8 mg of the sample was used for acquiring the experimental data. The test cell was sealed manually by a special tool equipped with Mettler's DSC, and we conducted dynamic scanning by starting the programmed setting. The DSC test was established as follows:

The β was selected to be 1, 2, 4, and $10\text{ }^\circ\text{C min}^{-1}$ by DSC in this study. The β was used as low rate; the reaction could be detected at a lower temperature. At the same time, if the β was employed as high rate by DSC, then the T_0 determination could be delayed, and the maximum temperature (T_{max}) was high. As a result, if β increases, we could reach the following phenomena [16]:

- The temperature at which reaction begins increases with β .
- The exothermic T_{max} increases β .
- The temperature at which the completion of the curve reaction occurs increases with β .
- The measure of a T_{max} increases with β .

Test cell: These gold-plated high-pressure crucibles, which can be pressed together, have been very useful for safety investigation, but they can only be used for one measurement with a maximum pressure of 15 MPa. The lid is pressed onto the crucible with a pressure of about a ton, so that the seal tightens the crucible. A toggle press is used to close the crucible [17, 18].

The E_a can be calculated using the built-in model of DSC that can be described as Eqs. 3 and 4. The nth-order model equation compared with the Arrhenius method of the temperature function of the reaction rate constant is [19]

$$\frac{d\alpha}{dt} = k_0 \exp\left(-\frac{E_a}{RT}\right) (1 - \alpha)^n \quad (3)$$

$$\frac{d\alpha}{dt} = H/A_{\text{tot}} \quad (4)$$

where H is the DSC signal deviation from baseline, and A_{tot} is the total peak area.

Thermal safety software

The TSS includes three groups of the program that correspond to a three-stage approach. We fully exploited the LTE model of ConvEx ForK (CE-FK) on the TSS to simulate a thermal explosion on a barrel. Here, CE-FK provided a numerical simulation of thermal explosion development. These simulative data were necessary for proper choice of safe conditions in application, such as storage and transportation, specifically for an energetic

chemical of interest [12]. The reaction mechanism of DCPO could be represented by the following kinetic model.

Initiation reaction:



Equation 5 can be described as n-order reaction.

where A is a reactant of reaction that was designed as DCPO; B is the product of reaction.

Equation 6 is the Arrhenius equation [20].

$$k = A \exp\left(-\frac{E_a}{RT}\right) \quad (6)$$

where k is the reaction rate, and E_a is the activation energy.

Equation 6 can be described as Eq. 7 in the chemical reaction. The k is equal to $d\alpha dt^{-1}$ in Eq. 7.

$$\frac{d\alpha}{dt} = k_0 \exp\left(-\frac{E_a}{RT}\right) (1 - \alpha)^n \quad (7)$$

where α is the conversion rate, and k_0 is the reaction rate of initiation. The n is reaction order in Eq. 7. Based on the experimental data, the thermokinetic parameters including 30 s^{-1} of k_0 , 1 of n , 740 J g^{-1} of Q , and 132 kJ mol^{-1} of E_a could be applied to simulate the thermal explosions under running with the software CE-FK on the TSS from CISP [12].

Thermal explosion simulation

The simulation project in STE and LET consists of three main parts:

- (1) The configuration and dimensions of a vessel, physical properties of a reacting liquid and material of the vessel's shell, and initial temperatures of shell and liquid;
- (2) Boundary conditions that define the type of heat exchange between the vessel and the environment;
- (3) Reaction kinetics.

Various vessel types (Table 2) were selected for simulation; as such, a tank is suitable for use in practice. STE

and LTE allow specifying boundary conditions of the first (Eq. 8), second (Eq. 9), and third type (Eq. 10). They are assumed to be uniform over each reactor surface and can be specified for each surface separately.

Boundary conditions of the first type (1st):

$$T_{\text{wall}} = g_1(t) \quad (8)$$

where $g_1(t)$ denotes a function that gives the time dependence of temperature on the wall.

Boundary conditions of the second type (2nd):

$$q_{\text{wall}} = -\lambda \frac{\partial T}{\partial r_{\text{wall}}} = g_2(t) \quad (9)$$

where $g_2(t)$ represents a function that gives the time dependence of heat flux on the wall.

Boundary conditions of the third type (3rd):

$$q_{\text{wall}} = -\lambda \frac{\partial T}{\partial r_{\text{wall}}} = g_1(t)(T_{\text{wall}} - g_2(t)) \quad (10)$$

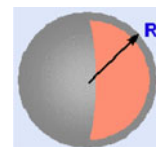
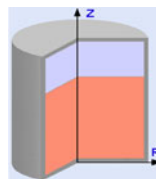
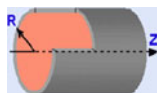
where $g_1(t)$ and $g_2(t)$ are the functions that provide the time dependence of the heat transfer coefficient and of the ambient temperature, respectively [14].

This study simulated various conditions for the barrel, such as normal storage at $40 \text{ }^\circ\text{C}$, runaway reaction temperature condition at $60 \text{ }^\circ\text{C}$, early step of external fire circumstance at $120 \text{ }^\circ\text{C}$, and fire conditions at $250 \text{ }^\circ\text{C}$. At storage, the ambient temperature will be equivalent to room temperature ($30\text{--}40 \text{ }^\circ\text{C}$ for summer); the heat transfer coefficient (HTC) for a barrel staying outdoors without wind was about $10 \text{ W m}^{-2} \text{ K}^{-1}$. If we were to evaluate accidental fire conditions, then the ambient temperature would be much higher than the cooling failure and the HTC might also be higher, because, in this case, air moves around the barrel. We took a temperature of about $250\text{--}300 \text{ }^\circ\text{C}$ and HTC of about $20 \text{ W m}^{-2} \text{ K}^{-1}$ to simulate the fire condition [14].

We divided the barrel into three surfaces: top, side, and bottom. The boundary conditions on the side and top surfaces were assumed to be of the third type. In practice, the barrel is built on the ground, so that the bottom is in close contact with the ground. Thus, it was reasonable to define

Table 2 Boundary parameter of CE-FK by various scenarios [14]

Vessel geometry



Dimension

Infinite cylinder $Z > 10R$

Barrel R, Z

Sphere R

conditions of the first type and take its temperature equal to the ambient one [14].

It should be noted that the simulation was carried out by assuming that the influence of the shell could be negligible. The kinetic model created on the basis of the DSC data completes the project. As the thermokinetic parameters are listed in this study, the model was transported from the ForK database.

Results and discussion

Thermal hazard analyses and thermal explosion simulation of DCPO

In order to determine the thermal hazard of 99.3 mass% DCPO, DSC under various heating rates was applied to determine the thermokinetics, as illustrated in Table 3. Table 3 shows a comparison of thermal curves of decomposition of 99.3 mass% DCPO with four types of β ($\beta = 1, 2, 4, \text{ and } 10 \text{ } ^\circ\text{C min}^{-1}$) by DSC. The initial reaction of DCPO was endothermic when temperature exceeded $40 \text{ } ^\circ\text{C}$, which caused a phase change at that moment.

Therefore, DCPO was stored indoors without sunshine. When the β value was lower, the decomposition reaction could be detected at a lower temperature. On the other hand, if β value was higher, then the T_0 determined could delay decomposition, and the T_{max} was correspondingly higher. DCPO decomposed at ca. $110 \text{ } ^\circ\text{C}$. Table 3 displays thermokinetic data and safety parameters of 99.3 mass% DCPO, which were obtained using STAR^e program of DSC. T_0 of DCPO was about $110 \text{ } ^\circ\text{C}$. In accordance with the experimental results, the reaction model was identified as an n-order reaction.

The E_a was estimated at 132 kJ mol^{-1} using STAR^e program of DSC. As a result, a rapid temperature increase of DCPO may cause a dramatic decomposition reaction under external fire conditions. Tables 3 were used for STE and LTE simulation. The aim of STE simulation was to determine a package of solid at the environmental temperature.

According to the recommendations on the Transport of Dangerous Goods, Manual of Tests and Criteria (TDG) of

Table 3 ForK simulation data compared with DSC experimental results of 99.3 mass% DCPO

Sample data		Experiment		Simulation	
$\beta/^\circ\text{C min}^{-1}$	Mass/mg	$T_0/^\circ\text{C}$	$\Delta H_d/\text{J g}^{-1}$	$T_0/^\circ\text{C}$	$\Delta H_d/\text{J g}^{-1}$
1	5.52	107	666	104	679
2	5.64	110	704	108	698
4	6.02	112	741	110	735
10	5.18	120	813	116	800

the United Nations (UN), the self-accelerating decomposition temperature (SADT) is defined as the lowest ambient temperature at which self-accelerating decomposition may occur in organic peroxides or self-reactive substances in the packaging for transportation purposes [20–24].

The SADT is the lowest environmental temperature (T_e) at which the temperature increase of a chemical substance is at least $6 \text{ } ^\circ\text{C}$ in a specified commercial package during a period of seven days or less.

The SADT of DCPO was calculated to be $66 \text{ } ^\circ\text{C}$ in TSS. All industrial users, producers, or transporters must well control storage temperature under SADT. Critical temperature (T_c) was defined as the system emergency temperature. If the controlling temperature exceeds T_c , then the system will arrive at an unstable situation and build up an early-step explosion. T_c was determined to be $69 \text{ } ^\circ\text{C}$ in

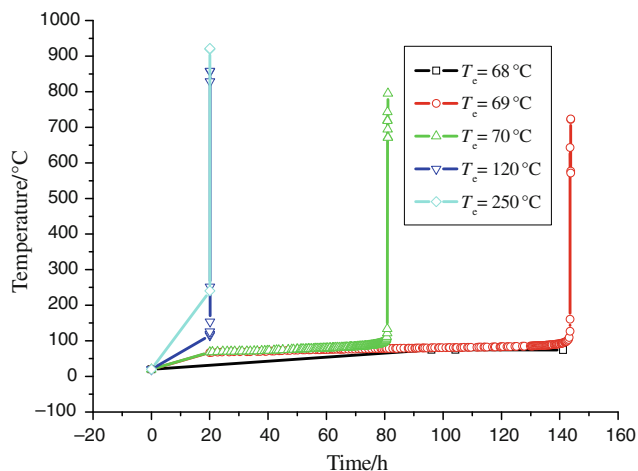


Fig. 1 Time versus temperature for STE of 99.3 mass% DCPO under various T_e

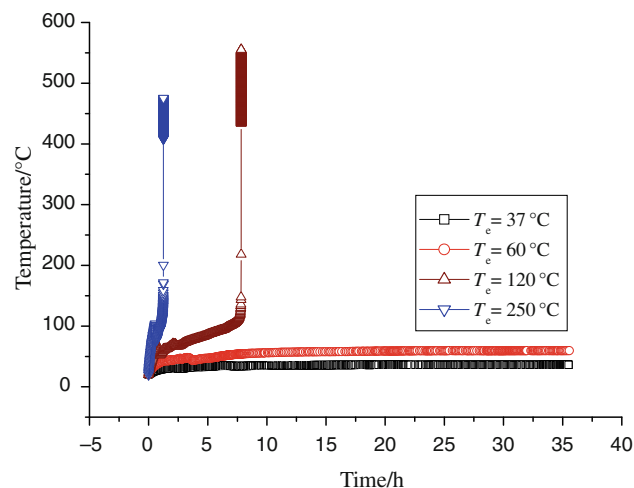


Fig. 2 Time versus temperature for LTE of 99.3 mass% DCPO under various T_e

TSS. A process safety engineer must understand T_c and control the reactor or storage tank, keeping away from T_c .

Figure 1 displays STE simulation by TSS. Environmental temperature in the range of 37–68 °C was analyzed without explosion development, because the system was not exceeding T_c . The system was exceeding SADT (66 °C), and so the system was accumulating heat. In parallel, T_e was set up at 69 °C in STE, and an explosion time resulted in 140 h. An explosion time at 70 °C of T_e was analyzed as 80 h in STE. At T_e values of 120 and 250 °C (fire situation) in STE, the corresponding explosion times were analyzed as 20 h. According to Fig. 1, STE was provided to operators for safe storage conditions.

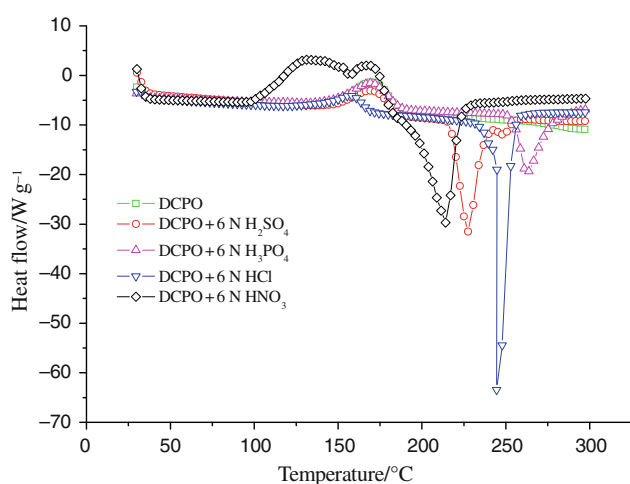


Fig. 3 Reactive hazard analyses of 99.3 mass% DCPO mixed with various acids by DSC under 4 °C min⁻¹ of β

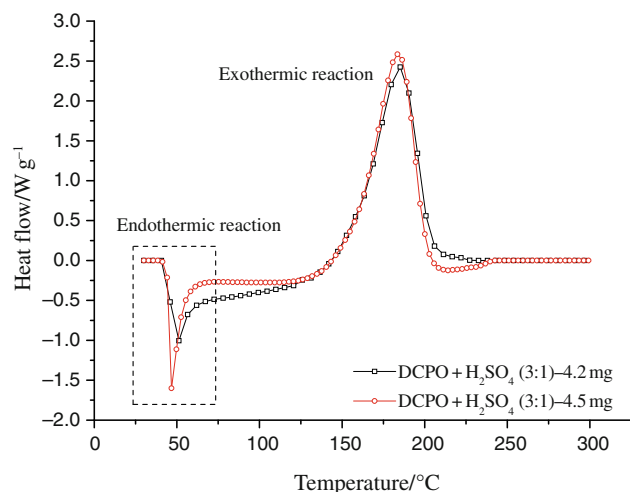


Fig. 4 Reactive hazard analyses and repeatability tests of 99.3 mass% DCPO mixed with 6 N H₂SO₄ by DSC under 10 °C min⁻¹ of β

Figure 2 shows LTE simulation under various values of T_e by TSS. We simulated four T_e situations: room temperature (37 °C), cooling system failure (60 °C), runaway reaction situation (120 °C), and external fire condition (250 °C) of DCPO stored in a storage tank (height 1.0 m and radius 0.5 m). In cooling failure condition, the ambient temperature equals room temperature (30–37 °C in summer in Taiwan), and the HTC for a barrel staying outdoors with no wind was about 10 W m² K⁻¹. If we analyzed accidental fire exposure, then the ambient temperature would be much higher than cooling failure, and the HTC might also be higher, because, in this case, air moves around the drum. We took a temperature of 250–300 °C for

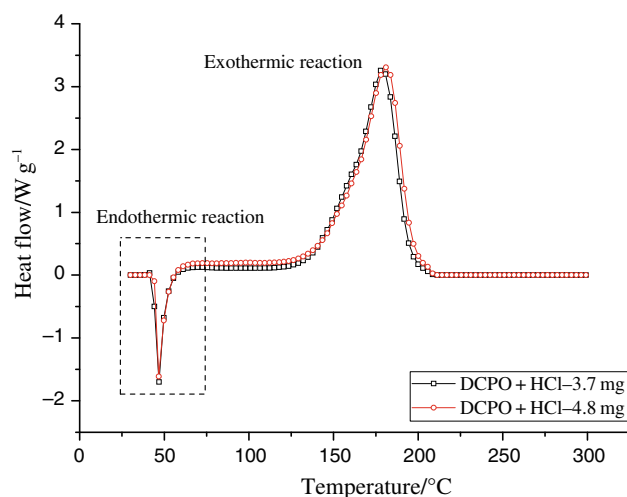


Fig. 5 Reactive hazard analyses and repeatability tests of 99.3 mass% DCPO mixed with 6 N HCl by DSC under 10 °C min⁻¹ of β

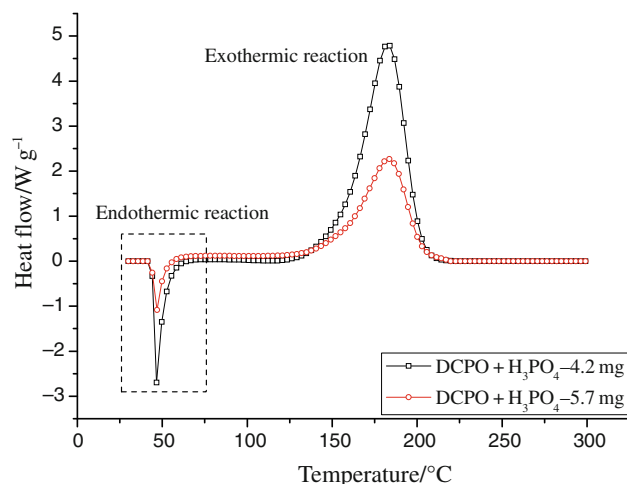


Fig. 6 Reactive hazard analyses and repeatability tests of 99.3 mass% DCPO mixed with 6 N HNO₃ by DSC under 10 °C min⁻¹ of β

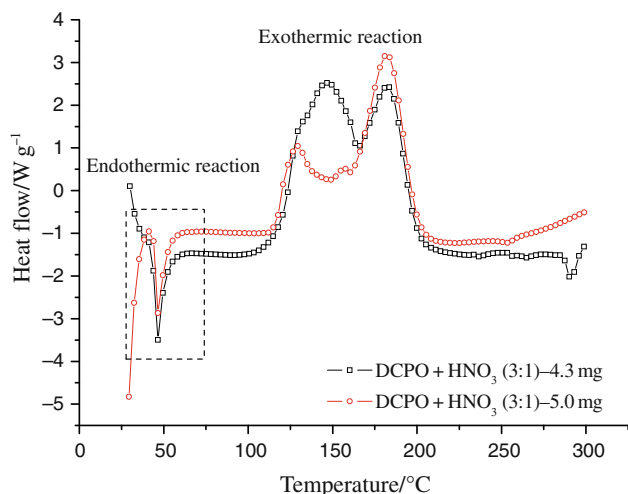


Fig. 7 Reactive hazard analyses and repeatability tests of 99.3 mass% DCPO mixed with 6 N H_3PO_4 by DSC under $10\text{ }^\circ\text{C min}^{-1}$ of β

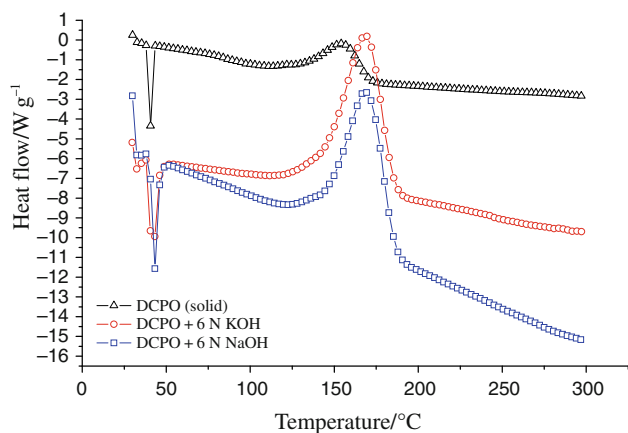


Fig. 8 Reactive hazard analyses of 99.3 mass% DCPO mixed with KOH and NaOH by DSC under $4\text{ }^\circ\text{C min}^{-1}$ of β

the fire exposure condition, and HTC could be taken at about $20\text{ W m}^2\text{ K}^{-1}$.

The T_e at $37\text{ }^\circ\text{C}$ was analyzed as the stable situation for a storage tank. The T_e at $60\text{ }^\circ\text{C}$ was determined as the stable condition without any runaway reaction for a storage

tank. When T_e was at $120\text{ }^\circ\text{C}$ in LTE, the emergency response time was 8 h. In this case, T_e was used at $250\text{ }^\circ\text{C}$ (fire situation) in LTE; the emergency response time was less than 2 h.

Reactive hazard evaluation of DCPO mixed with four typical acids and two fundamental bases

DCPO mixed with various acids are indicated in Fig. 3. An endothermic reaction at $160\text{ }^\circ\text{C}$ was discovered when DCPO was mixed with various acids. The thermal hazard of DCPO mixed with HNO_3 was more dangerous than with H_2SO_4 , HCl , and H_3PO_4 . The T_0 and ΔH_d of DCPO mixed with 6 N HNO_3 were calculated to be $70\text{ }^\circ\text{C}$ and 911 J g^{-1} , respectively. In order to avoid a thermal runaway reaction and thermal explosion of DCPO in storage area or reactor, DCPO must not be mixed with acids. Figures 4, 5, 6, and 7, respectively, describe the results of the repetition tests of DCPO mixed with four typical acids, H_2SO_4 , HCl , H_3PO_4 , and HNO_3 , by DSC using $10\text{ }^\circ\text{C min}^{-1}$ of β .

According to thermal curves from DSC tests, acid mixed with DCPO was discovered during the two steps including an endothermic reaction and an exothermic reaction. In fact, the endothermic reaction is the phase change (solid to liquid) of reaction. Therefore, the structure of DCPO was not attacked by acid under low temperature. However, acid attacked the structure of DCPO exceeding $100\text{ }^\circ\text{C}$ and caused the ΔH_d rising. The T_{max} of mixtures was shifted to $180\text{--}200\text{ }^\circ\text{C}$. Results showed that the structure of DCPO was changed in compatible reaction. The ΔH_d of DCPO compared with H_2SO_4 was calculated to be 496 (test 1) and 500 J g^{-1} (test 2) in Fig. 4. The ΔH_d of DCPO mixed with HCl was determined to be 595 (test 1) and 567 J g^{-1} (test 2) as shown in Fig. 5. On the other hand, the process engineers must take care of HNO_3 in chemical industries. HNO_3 caused terrible reaction with the ΔH_d of mixtures increasing to $1,000\text{ J g}^{-1}$.

This study was applied to assess the thermal hazard of DCPO mixed with acids or bases in industry. Thermal hazards of DCPO mixed with 6 N KOH or NaOH were evaluated and are shown in Fig. 8. Thermokinetics of DCPO compared with acids or bases are displayed in Table 4.

Table 4 Thermal hazard of DCPO mixed with various acids or bases by DSC under $4\text{ }^\circ\text{C min}^{-1}$ of β

Material	Mass ratio	$T_0/^\circ\text{C}$	$\Delta H_d/\text{J g}^{-1}$	$\Delta H_{\text{endo}}/\text{J g}^{-1}$	$E_a/\text{kJ mol}$	$\ln(k_0)/\text{s}^{-1}$
DCPO	NA	110	736	NA	117	26
DCPO + 6 N HCl	3:1	110	163	874	106	24
DCPO + 6 N H_3PO_4	3:1	110	245	319	147	34
DCPO + 6 N HNO_3	3:1	70	911	502	33	4
DCPO + 6 N H_2SO_4	3:1	110	285	670	150	35
DCPO + 6 N NaOH	3:1	110	386	NA	138	32
DCPO + 6 N KOH	3:1	110	337	NA	143	33

Conclusions

As a result of this study, five conclusions were reached as follows:

- A kinetics-based simulation is valuable for determining the self-heating rate. In practice, numerical simulation is a unique way to understand the thermal hazards of reactive chemicals. As far as the degree of hazard under runaways, our results from curve fitting and experimental data provided evidence to show that the degree of hazard for DCPO significantly increased when the concentration increased.
- Thermokinetics determined from the thermal curves could be employed to assess the thermal explosion hazard of OPs of interest and to evaluate safety parameters, such as T_0 , temperature of no return (T_{NR}), and SADT.
- When properly maintained at low temperature during transportation and storage, the refined DCPO, a white crystalline solid product, will not initiate any prominent runaway reaction, unless it goes through the melting stage under high temperature. However, it is likely to result in accidents in a chemical process under conditions of higher temperature, incompatible substances, improper temperature control, or human error.
- The DCPO is a white solid that decomposes at 30–40 °C (solid to liquid). DCPO products must be stored at room temperature (indoor) without exposure to sunshine. DCPO decomposes at 110 °C (thermal runaway reaction). The temperature setting for an alarm was applied at 70 °C in a batch reactor. In practice, these data are necessary for safe conditions of application, storage, and transportation of a reactive chemical. Future studies will focus on the reaction mechanism of DCPO analysis in a batch reactor. Finally, the model program could fit or simulate the experimental data and the real case, which can save time and money without loss of safety, to evaluate the severity of hazards of energetic chemicals.
- Thermal hazard of DCPO mixed with HNO_3 was more dangerous than when it was mixed with H_2SO_4 , HCl , and H_3PO_4 . For DCPO mixed with 6 N HNO_3 , T_0 was calculated to be 70 °C by DSC, ΔH_d was determined to be 911 J g⁻¹ and E_a was calculated to be 33 kJ mol⁻¹.

Acknowledgements The authors would like to thank Dr. Houn-Yi Hou for his valuable suggestions on experiments and measurements of runaway reactions. The authors are grateful to the supplier for professional operating techniques and information. In addition, the authors appreciate the technical assistance provided by Dr. Arcady A. Kossoy of ChemInform Saint Petersburg (CISP), Ltd., St. Petersburg, Russia, and Mr. Anthony M. Janeshek, senior specialist of Dow Chemical, Freeport, Texas, USA.

References

1. Duh YS, Kao CS, Hwang HH, Lee WL. Thermal decomposition kinetics of cumene hydroperoxide from the cumene oxidation process. *Trans Inst Chem Eng.* 1998;76(Part B):271–6.
2. Duh YS, Kao CS, Lee C, Yu SW. Runaway hazard assessment of cumene hydroperoxide from the cumene oxidation process. *Trans Inst Chem Eng.* 1997;75:73–80.
3. Fisher HG, Goetz DD. Determination of self-accelerating decomposition temperatures for self-reactive substances. *J Loss Prev Process Ind.* 1993;6(3):305–16.
4. Wu KW, Hou HY, Shu CM. Thermal phenomena studies for dicumyl peroxide at various concentrations by DSC. *J Therm Anal Calorim.* 2006;83:41–4.
5. Wang YW, Duh YS, Shu CM. Evaluation of adiabatic runaway reaction and vent sizing for emergency relief from DSC. *J Therm Anal Calorim.* 2006;85:225–34.
6. Yeh PY, Shu CM, Duh YS. Thermal hazard analysis of methyl ethyl ketone peroxide. *Ind Eng Chem Res.* 2003;42(1):1–5.
7. Chang RH, Tseng JM, Jehng JM, Shu CM, Hou HY. Thermokinetic model simulations for methyl ethyl ketone peroxide contaminated with H_2SO_4 or NaOH by DSC and VSP2. *J Therm Anal Calorim.* 2006;83:57–62.
8. Tseng JM, Chang RH, Horng JJ, Chang MK, Shu CM. Thermal hazard evaluation for methyl ethyl ketone peroxide mixed with inorganic acids. *J Therm Anal Calorim.* 2006;85:189–94.
9. Tseng JM, Chang YY, Su TS, Shu CM. Study of thermal decomposition of methyl ethyl ketone peroxide using DSC and simulation. *J Hazard Mater.* 2007;142:765–70.
10. Chen JR, Wu SH, Lin SY, Hou HY, Shu CM. Utilization of microcalorimetry for an assessment of the potential for a runaway decomposition of cumene hydroperoxide at low temperatures. *J Therm Anal Calorim.* 2008;93:127–33.
11. Wu SH, Wang YW, Wu TC, Hu WN, Shu CM. Evaluation of thermal hazards for dicumyl peroxide by DSC and VSP2. *J Therm Anal Calorim.* 2008;93:189–94.
12. Chen KY, Wu SH, Wang YW, Shu CM. Runaway reaction and thermal hazards simulation of cumene hydroperoxide by DSC. *J Loss Prev Process Ind.* 2008;21:101–9.
13. Wang WY, Shu CM, Duh YS, Kao CS. Thermal runaway hazards of cumene hydroperoxide with contaminants. *Ind Eng Chem Res.* 2001;40:1125–34.
14. You ML, Liu MY, Wu SH, Chi JH, Shu CM. Thermal explosion and runaway reaction simulation of lauroyl peroxide by DSC tests. *J Therm Anal Calorim.* 2009;96:777–82.
15. Chen YL, Chou YP, Hou HY, YP I, Shu CM. Reaction hazard analysis for cumene hydroperoxide with sodium hydroxide or sulfuric acid. *J Therm Anal Calorim.* 2009;95(2):535–9.
16. Lin WH, Wu SH, Shiu GY, Shieh SS, Shu CM. Self-accelerating decomposition temperature (SADT) calculation of methyl ethyl ketone peroxide using an adiabatic calorimeter and model. *J Therm Anal Calorim.* 2009;95(2):645–51.
17. Ando T, Fujimoto T, Morisaki S. Analysis of differential scanning calorimetric data for reactive chemical. *J Hazard Mater.* 1991;251–80.
18. Maria G, Heinze E. Kinetic system identification by using short-cut techniques in early safety assessment of chemical processes. *J Loss Prev Process Ind.* 1998;11:187–206.
19. STAR[®]. Software with Solaris Operating System, Operating Instructions, Mettler Toledo, Switzerland; 2008.
20. Yu Y, Hasegawa K. Derivation of the self-accelerating decomposition temperature for self-reactive substances using isothermal calorimeter. *J Hazard Mater.* 1996;45:193–205.

21. Recommendations on the Transport of Dangerous Goods. Manual of Tests and Criteria. 4th revised ed. United Nations, ST/SG/AC.10/11/Rev. 4th, United Nations, New York, USA and Geneva, Switzerland; 2003.
22. Yang D, Koseki H, Hasegawa K. Predicting the self-accelerating decomposition temperature (SADT) of organic peroxides based on non-isothermal decomposition behavior. *J Loss Prev Process Ind.* 2003;16(5):411–6.
23. Semenov NN. Some problems of chemical kinetic and reactivity. Part II. London, UK: Pergamon Press; 1959.
24. Townsend DI, Tou JC. Thermal hazard evaluation by an accelerating rate calorimeter. *Thermochim Acta.* 1980;37:1–30.